



# 1 Harmonising and mapping Patagonian Shelf seabed sediment data

2

3 Zoë A. Roseby<sup>1</sup>, Sophie L. Ward<sup>2</sup>, Torsa Sengupta<sup>1</sup>, Callum M. Roberts<sup>3</sup>, James D. Scourse<sup>1</sup>

4

5 <sup>1</sup> Department of Earth and Environmental Sciences, University of Exeter, Penryn Campus, Penryn, Cornwall, UK, TR10  
6 9FE.

7 <sup>2</sup> School of Ocean Sciences, Bangor University, Menai Bridge, Isle of Anglesey, Wales, UK, LL59 5AB.

8 <sup>3</sup> Centre for Ecology and Conservation, University of Exeter, Penryn Campus, Penryn, Cornwall, UK, TR10 9FE.

9

10 *Correspondence to:* Zoë A. Roseby (Z.Roseby@exeter.ac.uk)

11

12 **Abstract.** Maps of seabed sediment distribution on global continental shelves are useful for a wide range of applications,  
13 including for habitat mapping, predicting sedimentary carbon stocks, and providing insight into past and present  
14 oceanographic conditions and the processes influencing sediment transport and deposition. Whilst some continental shelves  
15 have relatively well mapped seabed sediments, others lack publicly available, harmonised datasets. The Patagonian Shelf,  
16 also known as the Argentine Shelf, is one of the world's largest continental shelves, but there is currently no database that  
17 has compiled publicly available seabed sediment data. In this paper we collate and harmonise existing published and open-  
18 access seabed grain size data for the Patagonian Shelf. The paper combines both quantitative and qualitative data from  
19 published and grey literature and translates these data into two modified Folk sediment classification schemes. Ordinary  
20 Kriging is used to map the spatial distribution of different sediment classes across the shelf and allows us to assess  
21 uncertainty in the predictions of seabed sediment type. Overall, our sediment maps agree well with previously published  
22 maps over the central and northern shelf. Key differences are the classification of shell-rich sediments, and the spatial  
23 distribution of coarse sediments, particularly over the southern shelf. The latter would be further resolved with greater  
24 sampling of seabed sediments in the region. The data products produced for this study are grain size point data for the shelf  
25 and interpolated Geographic Information System (GIS) layers of seabed sediments and associated prediction errors. These  
26 are freely available for download via Zenodo (Roseby et al., 2026; <https://doi.org/10.5281/zenodo.19111158>).

27

## 28 1. Introduction

29 Maps of seabed sediment distribution on global continental shelves are useful for a variety of purposes. For example, an  
30 understanding of surficial sediment type is important for habitat mapping (Robinson et al., 2011), predicting sedimentary  
31 carbon stocks (Diesing et al., 2021, 2024; Smeaton et al., 2021) and can provide insights into past and present



32 oceanographic conditions and the processes influencing sediment transport and deposition (Ward et al., 2025). Whilst some  
33 continental shelves have relatively well mapped seabed sediments, amongst them the Northwest European Shelf (e.g.  
34 Kaskela et al., 2019), others lack publicly available, harmonised datasets.

35

36 The Patagonian Shelf, also known as the Argentine Shelf, is one of the world's largest continental shelves, covering 9.6  
37 million km<sup>2</sup> (Violante et al., 2014; Fig.1). Extensive research on sediment distribution on the shelf has been conducted over  
38 the 20<sup>th</sup> and 21<sup>st</sup> Centuries. In the late 1950's and early 1960's the Lamont-Doherty Earth Observatory recovered ~170  
39 piston cores from the shelf via the research vessel *Vema*, providing insight into the shelf lithology (Fray and Ewing, 1963;  
40 Guilderson et al., 2000). Other work has published detailed seabed sediment maps for specific sub-regions of the shelf  
41 (Parker et al., 1982; Mouzo and Paterlini, 2017) or provided an overview of sediment type for the entire shelf (Parker et  
42 al., 1996, 1997; Violante et al., 2014). Publicly available point observations of surficial sediments and grain size data  
43 originate from several additional studies (Boosman, 1973; Richards and Dzwilewski, 1974; Roux and Bremex, 1996;  
44 Fernandez, 2006; Bernasconi and Cusminsky, 2009; Lantzsch et al., 2014; Moreira et al., 2016; Tuduri et al., 2018; Ronda  
45 et al., 2019; Oliva et al., 2020; Doldan et al., 2021; Chaparro et al., 2022; Desiage et al., 2023).

46

47 Despite this broad understanding of the large-scale distribution of sediments on the Patagonian Shelf (e.g. Violante et al.,  
48 2014), and availability of detailed regional case studies, there is currently no open database that has compiled publicly  
49 available seabed sediment data from across the shelf. Furthermore, existing maps do not appear in a format which can be  
50 easily incorporated into Geographic Information System (GIS) software. This paper outlines the steps taken to collate and  
51 harmonise existing open-access seabed grain size data for the shelf. These steps include the collation of both quantitative  
52 and qualitative sediment data from published and grey literature, and the translation of these data into two modified Folk  
53 schemes (Folk, 1954; Kaskela et al., 2019; Smeaton et al., 2021). The data products produced for this study are grain size  
54 point data for the shelf and interpolated Geographic Information System (GIS) layers of seabed sediments and associated  
55 prediction errors.

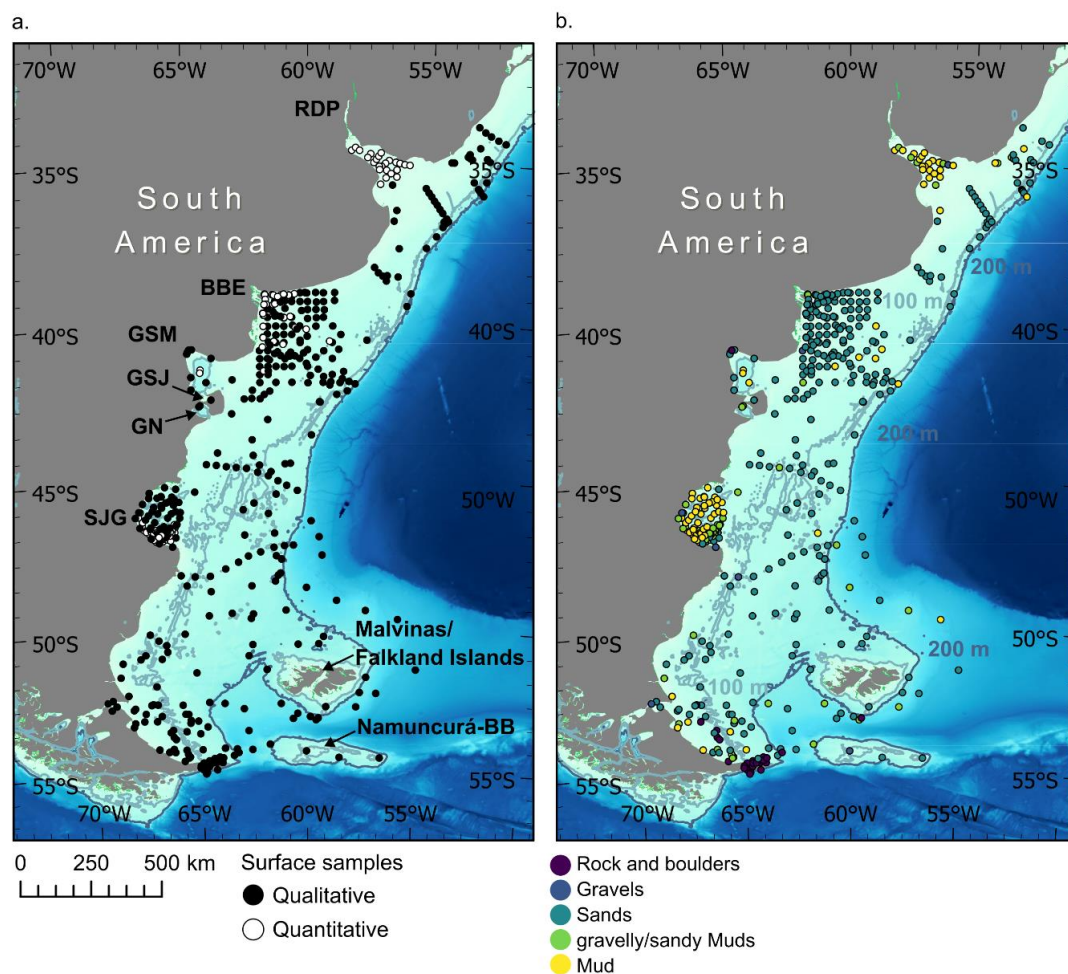
56

## 57 **2. Regional Setting**

58 The Patagonian Shelf is ~2,400 km long and oriented approximately north-east to south-west. It has an average width of  
59 400 km, varying between 170 and 850 km (Fig. 1a; Violante et al., 2014 and references therein). With water depths typically  
60 less than 150 m (average depth is 115 m), much of the continental shelf was exposed during Pleistocene sea-level lowstands  
61 (Guilderson et al., 2000; Violante and Parker, 2004). Past cycles of shelf exposure and flooding have greatly influenced  
62 the shelf lithology and bathymetry. The Patagonian Shelf is generally smooth but features four terraces, oriented north



63 north-east to south south-west, separated by high-gradient steps (Groeber, 1948; Parker et al., 1997; Violante et al., 2014).  
64 These terraces may be associated with interruptions in sea-level rise during past marine transgressions, that led to cliff-like  
65 erosional features to form at the palaeo-shoreline (Perillo et al., 2005; Violante, 2005; Ponce et al., 2011).  
66



67  
68 **Figure 1:** Map of the Patagonian Shelf with graduated colour and contours indicating shelf bathymetry. Bathymetry is from  
69 GEBCO Compilation Group (2024). Compiled sediment samples are shown, with colour indicating (a) whether the sediment  
70 data at that site are quantitative or qualitative and (b) seabed sediment type based on a five class modified Folk scheme (Folk-5;  
71 Fig. 2). Locations noted in the text are indicated: Río de la Plata estuary (RDP), Bahía Blanca Estuary (BBE), Golfo San Matías  
72 (GSM), Golfo San José (GSJ), Golfo Nuevo (GN) San Jorge Gulf (SJG), and Namuncurá-Burdwood Bank (Namuncurá-BB).  
73



74 Dominant sources of sediment to the shelf are the Andean region and the Brazilian Shield (Depetris and Griffin, 1968;  
75 Potter, 1994; de Mahiques et al., 2008; Violante et al., 2014), introduced through coastal erosion, and fluvial and aeolian  
76 transport (Violante et al., 2014). Sediments are predominantly terrigenous, eroded from the land, and composed of silicate  
77 minerals. The shelf seabed is dominated by sands (fine to medium grained quartz), with accumulations of mud within  
78 sheltered coastal regions including within Río de la Plata estuary, the Bahía Blanca estuary, Golfo San Matías, Golfo San  
79 José, Golfo Neuvo, Golfo San Jorge and the inner Patagonian Shelf south of Golfo San Jorge (Fray and Ewing, 1963;  
80 Parker et al., 1997; Violante et al., 2014). The extensive sand cover represents relict transgressive littoral barrier systems,  
81 formed during sea-level rise following the Last Glacial Maximum (26-21 ka BP; Violante and Parker, 2004; Clark et al.,  
82 2009). Gravels are found in patches, predominantly located along the southern Patagonian Shelf, with areas of shell hash  
83 towards the northern extent, seawards of Río de la Plata (Violante et al., 2014).

84

### 85 **3. Methods**

#### 86 **3.1 Data compilation and classification**

87 This study compiles archival surface sediment grain size data (both quantitative and qualitative) for the Patagonian Shelf  
88 from published literature, PhD theses and core repositories. Qualitative data are based on surface sediment descriptions,  
89 from a combination of grab, dredge and trawl samples, and the upper units of cores. Quantitative data are primarily based  
90 on sediment sieving and/or laser particle analysis. For this study, quantitative grain size data are reported as percentage  
91 gravel (> 2mm), sand (2-0.063 mm) and mud (<0.063 mm) based on the Folk classification scheme (Folk, 1954).

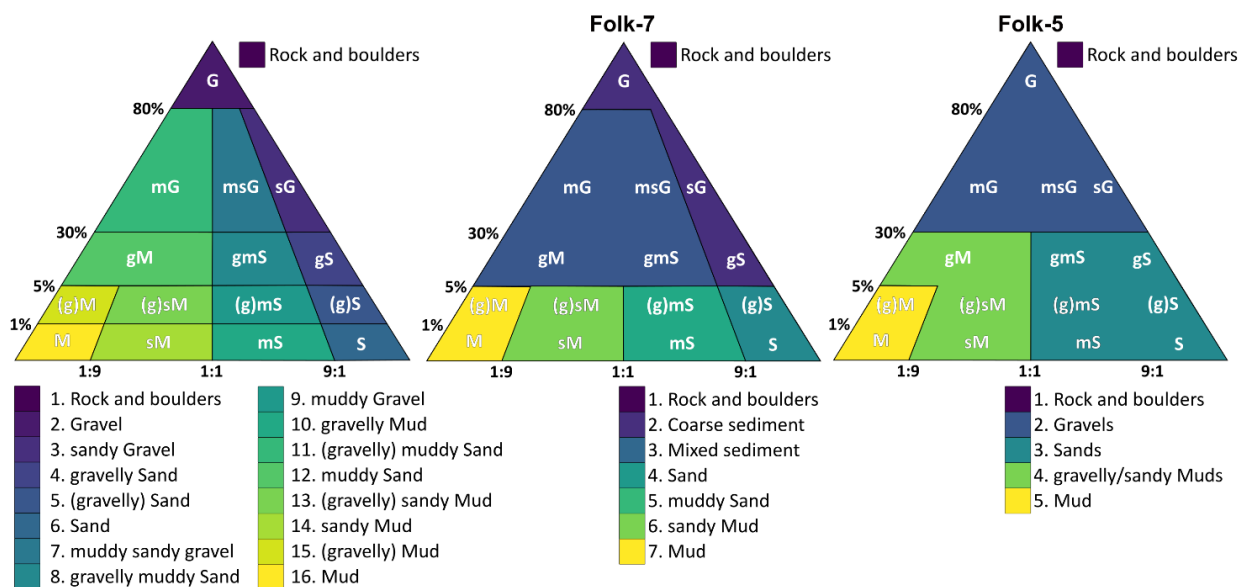
92

93 Kaskela et al. (2019) described the compilation and harmonisation of seabed sediment data for European seas. They utilised  
94 a modified Folk scheme to classify sediments, with three granularities of 16, 7 and 5 classes (Folk, 1954; Kaskela et al.,  
95 2019). We utilised a similar scheme here, altering the five-class division so that sediments with a high mud content (>90%)  
96 were in an isolated category (Fig. 2; Williams et al., 2019). Mud-rich sediments can act as a major sink for nutrients  
97 (including organic carbon) and pollutants (Palanques et al., 1990; Liu et al., 2011; de Mahiques et al., 2015; Atwood et al.,  
98 2020; Diesing et al., 2021; Smeaton et al., 2021). Furthermore, they form unique habitats with distinct benthic communities  
99 (e.g. JNCC, 2022). We therefore saw value in isolating this grain size category from sediments with a higher sand and  
100 gravel content (Fig. 2). We opted to exclude a 16-class scheme from the final dataset, based on the large qualitative  
101 component and uncertainty around translating sediment descriptions to such a fine granularity. Quantitative data was  
102 classified into a seven (Folk-7) or five (Folk-5) class scheme based on the percentage of gravel, sand and mud, whilst  
103 qualitative descriptions were translated using expert judgement (Fig. 2). The classification of qualitative descriptions was  
104 carried out by two independent researchers to improve reliability and validity of the categorisation process – any differences



105 in classification were discussed and resolved through consensus. In addition to the grain size categories shown in the Folk  
 106 triangle, both the Folk-7 and Folk-5 schemes include a rock and boulders category (Fig. 2).

107



108

109 **Figure 2: The Folk sediment triangle (left; Folk, 1954) and derived seven (Folk-7) and five class schemes (Folk-5; middle and**  
 110 **right, respectively) used in this study.**

111

### 112 3.2. Seabed sediment data interpolation

113 Following Smeaton and Austin (2019) and Smeaton et al. (2021), sediment descriptions were assigned a numerical value,  
 114 following the seven and five class schemes outlined in Figure 2. Data points were interpolated in ArcGIS Pro 3.0.1, with  
 115 the Exploratory Interpolation tool used to assess the performance of different interpolation techniques. For both the Folk-  
 116 5 and Folk-7 datasets, we assessed the accuracy of Universal Kriging (Optimised), Ordinary Kriging (Optimised), Simple  
 117 Kriging (Optimised) and Empirical Bayesian Kriging (Default). The statistical parameters considered were Mean Error,  
 118 Root-Mean-Square-Error (RMSE) and the coefficient of determination ( $R^2$ ), between the observed and predicted values  
 119 (e.g. Boumpoulis et al., 2023). A model that produces good predictions should have a small RMSE, which considers the  
 120 difference between the observed and predicted values, and a Mean Error close to 0, which demonstrates a lack of bias in  
 121 the prediction (Boumpoulis et al., 2023). A high  $R^2$  value indicates a good correlation between observed and predicted  
 122 values.

123



124 We defined a limit of the interpolated area between the coastline, and the 500 m shelf contour (Fig. 1a; GEBCO  
125 Compilation Group, 2024) and included coastal and inshore environments such as gulfs and estuaries. Whilst the shelf is  
126 typically shallower than 200 m, by extending the depth of interpolation to 500 m we incorporate Namuncurá-Burdwood  
127 Bank (Fig. 1a). This created a shelf area for analysis of 1.21 million km<sup>2</sup>.

128

129 The reclassify function in ArcGIS was used to ‘bin’ the interpolated surface, as the interpolation tool allowed for prediction  
130 across the 1-7 range when using the Folk-7 scheme, and the 1-5 range when using the Folk-5 scheme (Fig. 2). For example,  
131 when using the Folk-7 scheme, a pixel with a predicted value of 3.7 was binned into the 3.5-4.5 (Sand) category. The raster  
132 to polygon function was used to convert the reclassified raster layer into a vector format, so that the area of coverage per  
133 sediment type could be calculated. To calculate areal measurements in ArcGIS Pro, an Albers equal area conic projection  
134 for South America was used following Esri (2025). To assess uncertainty, a standard error of prediction surface was output  
135 from the interpolation tool.

136

#### 137 **4. Results**

138 A total of 486 surface samples were collated (Table 1), 380 (78%) of which were qualitative, and 106 (22%) of which were  
139 quantitative (Fig. 1). The mean distance between points (nearest neighbour) is 23 km, with a maximum distance of 163  
140 km. These data mostly come from published literature, PhD theses and from core logs provided by various core/data  
141 repositories, including Lamont-Doherty Earth Observatory, Byrd Polar and Climate Research Center and the Antarctic  
142 Core Collection at the Oregon State University Marine and Geology Repository. We found seven surface samples that we  
143 categorised as shell hash, which were not assigned a Folk code. Most shelly sediments are sands with shell fragments and  
144 are therefore categorised as ‘Sand’ or ‘(gravelly) Sand’ following Smeaton et al. (2021).

145

146 The Exploratory Interpolation tool in ArcGIS Pro was used to assess the performance of different interpolation techniques.  
147 When considering the outlined statistical parameters across all techniques, we find that Ordinary Kriging (Optimised)  
148 demonstrates a relatively low Root Mean Squared Error (RMSE), a Mean Error that indicates a lack of bias and satisfactory  
149 R<sup>2</sup> for both the Folk-5 and Folk-7 datasets (Table 2). We therefore use Ordinary Kriging to produce the interpolated  
150 sediment maps for this study (Fig. 3 and 4). The cell size of the output raster is 25 km<sup>2</sup>.

151

152

153

154



155 **Table 1: Data sources for Patagonian Shelf seabed sediment study. Laser Particle Size Analyser (LPSA), Grain Size Analysis**  
 156 **(GSA).**

Author/Repository	Sampling method	GSA method	No. samples
Bernasconi and Cusminsky (2009)	Piston Core	Description	2
Boosman (1973)	Grab	Description	91
Desiage et al. (2023)	Piston Core	Description	4
Doldan et al. (2021)	Observation	Description	8
Fernandez (2006)	Tube corers, spring corers, dredges, and trawls	Sieving	46
Fernandez (2006), Chaparro et al. (2022)	Tube corers, spring corers, dredges, and trawls	Sieving	39
Lantzsich et al. (2014)	Vibro Core	Description	10
Moreira et al. (2016), Tuduri et al. (2018)	Grab	LPSA	24
Oliva et al. (2020)	Grab	NA	27
Richards and Dzwilewski (1974)	Gravity core	ASTM D422-63	2
Ronda et al. (2019)	Dredge	LPSA	7
Roux and Bremec (1996)	NA	Description	27
<i>Repository: Lamont-Doherty Earth Observatory</i>	Piston core, grab, trawl	Description	167
<i>Repository: Byrd Polar and Climate Research Center</i>	Trawl, dredge, grab	Description	25
<i>Repository: Antarctic Core Collection</i>	Piston core, grab, dredge	Description	7
			<b>Total = 486</b>

157

158 **Table 2: Performance statistics of different interpolation techniques for the Folk-5 and Folk-7 datasets. For both the Folk-5 and**  
 159 **Folk-7 datasets, we assessed the accuracy of Universal Kriging (Optimised), Ordinary Kriging (Optimised, used here), Simple**  
 160 **Kriging (Optimised) and Empirical Bayesian (EB) Kriging (Default).**

	Folk-5				Folk-7			
	Universal	<b>Ordinary</b>	Simple	EB	Universal	<b>Ordinary</b>	Simple	EB
RMSE	0.643	<b>0.636</b>	0.634	0.652	1.075	<b>1.066</b>	1.072	1.083
Mean Error	-0.002	<b>0.000</b>	0.015	-0.009	-0.005	<b>0.001</b>	-0.034	-0.016
R <sup>2</sup>	0.603	<b>0.612</b>	0.614	0.597	0.565	<b>0.572</b>	0.568	0.563

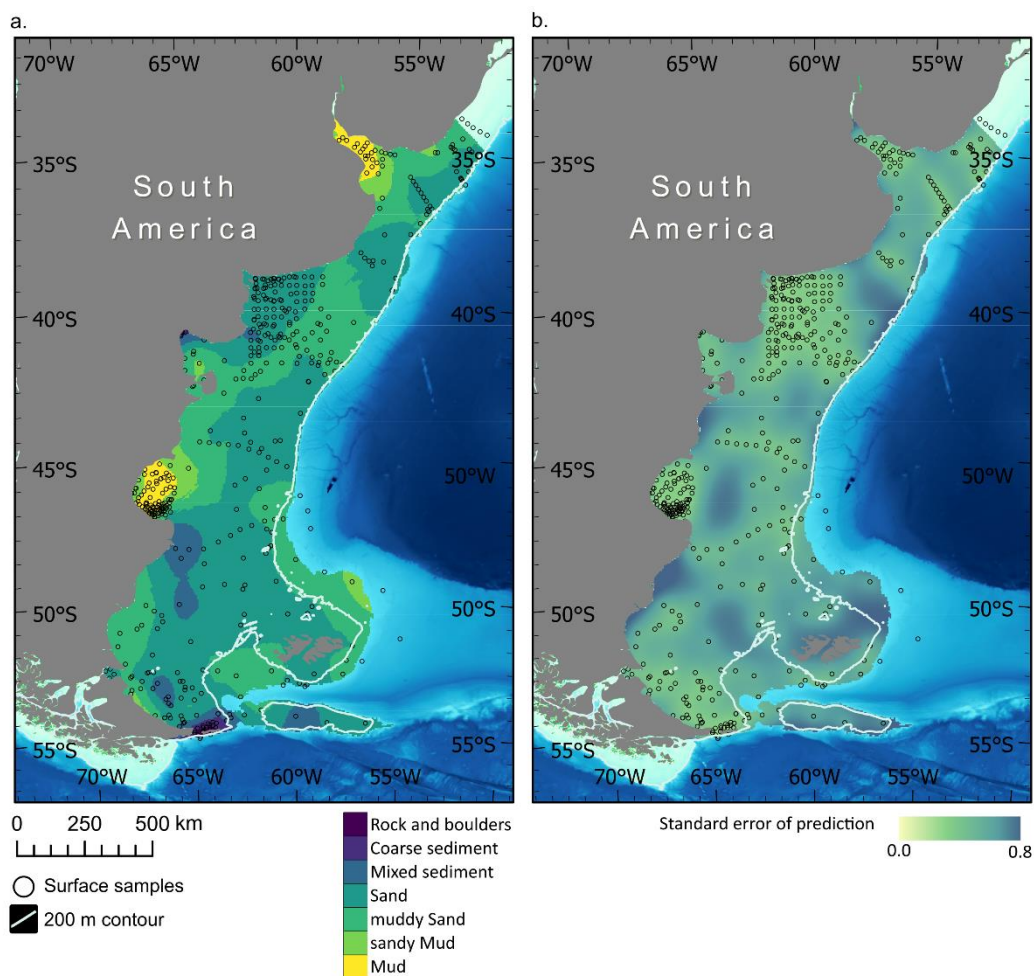
161

#### 162 **4.1. Spatial variability in sediment classification**

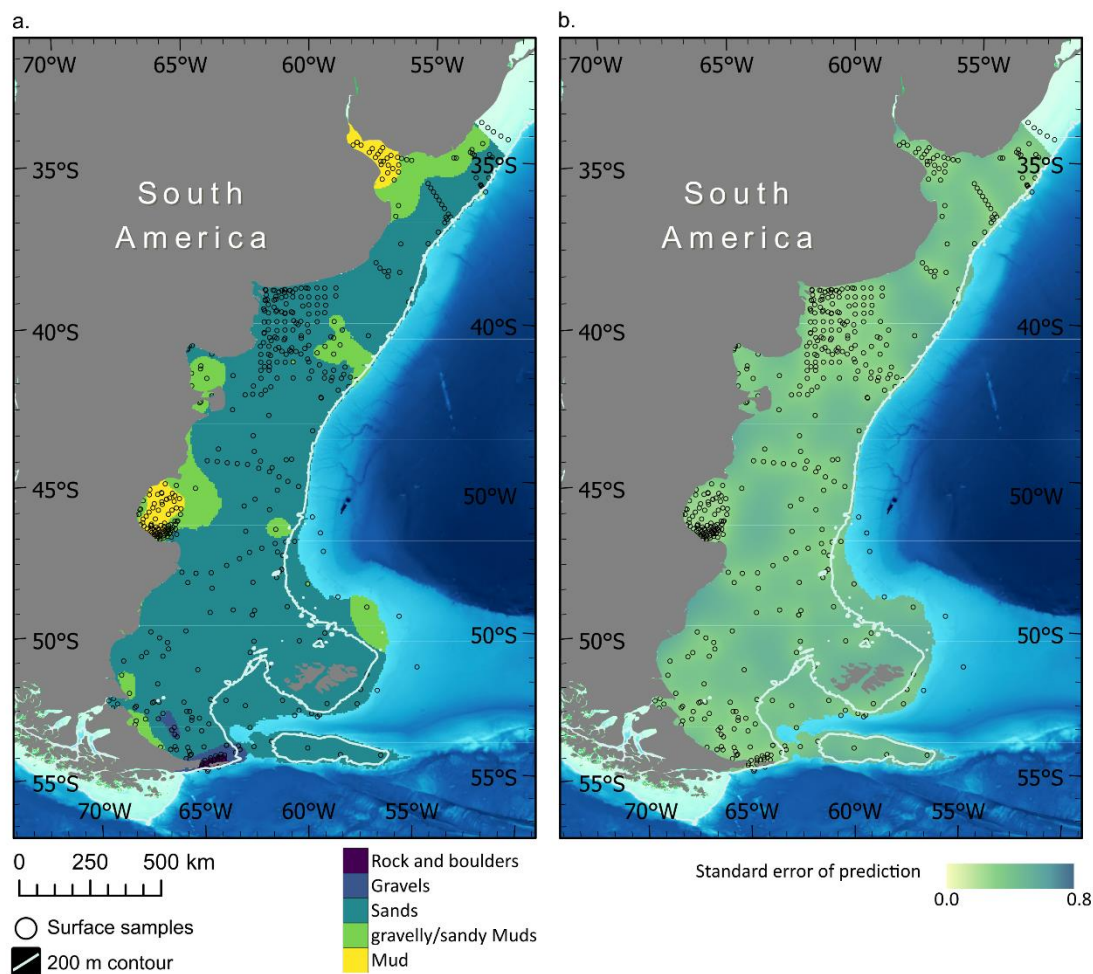
163 The general pattern of sediment distribution modelled for the Patagonian Shelf (Fig. 3a and 4a), largely reflects previously  
 164 published maps (Violante et al, 2014; modified after Parker et al., 1996). The shelf is dominated by sands, with lower  
 165 proportions of gravel, muds and rock/boulders (Fig. 5). Results of the Folk-7 interpolation indicate that 53% of the shelf is



166 comprised of Sand, 34% is muddy Sand, with only 4% and 3% of the shelf comprised of sandy Mud and Mud, respectively.  
167 Based on this scheme, 5% of the shelf sediments are Mixed and only 1% Coarse. For the Folk-5 scheme, where Sand and  
168 muddy Sand are combined, 83% of the area of the shelf falls into this category. 12% of sediments are gravelly/sandy Muds,  
169 with 3% of the shelf comprised of Mud. Only 1% of sediments are considered Gravel under the Folk-5 scheme.  
170



171  
172 **Figure 3: (a) Sediment map of the Patagonian Shelf classified using the 7-class Folk scheme, modelled with the Ordinary Kriging**  
173 **tool in ArcGIS Pro from archived surface sediment data (Table 1). (b) Map of standard error of prediction from Ordinary**  
174 **Kriging.**  
175



176

177 **Figure 4: (a) Sediment map of the Patagonian Shelf classified using the 5-class Folk scheme, modelled with the Ordinary Kriging**  
178 **tool in ArcGIS Pro from archived surface sediment data (Table 1). (b) Map of standard error of prediction from Ordinary**  
179 **Kriging.**

180

181 Violante et al. (2014; after Parker et al., 1997) show the areal coverage of sands on the shelf to be 65% and shells to be  
182 12.5%. As described above, here we categorise most shelly sediments as ‘Sand’ or ‘(gravelly) Sand’ (following Smeaton  
183 et al., 2021). This explains the greater proportion of the Patagonian Shelf substrates described as ‘Sandy’ (Folk-5: 83%) in  
184 this study, when compared to the earlier results (Parker 1997; Violante et al., 2014). We find that the spatial distribution of  
185 sands align with previous maps, present along the entire length of the shelf and dominant over the middle and outer shelf,  
186 particularly in the central and northern regions (Parker et al., 1996; Violante et al. 2014).



187

188 In this study, only 1-5% of sediments are described as Mixed or Coarse (which includes all sediment with a gravel  
189 component >5% under the Folk-7 scheme; Fig. 2) or Gravel (which includes Gravel, muddy Gravel, muddy sandy Gravel  
190 and sandy Gravel under the Folk-5 scheme; Fig.2), compared to 12.5% reported in earlier studies (Parker et al., 1997;  
191 Violante et al., 2014). Gravel is found in greater concentrations south of 46°S, associated with ancient fluvial and glacial-  
192 fluvial deposits (Violante et al., 2014). Whilst we also find that Mixed, Coarse and Gravelly sediments are predominantly  
193 found south of 46°S, we find that they cover a considerably smaller area. This may be due to the classifications used in this  
194 study, where some gravelly sediments are grouped into other categories. For example, under the Folk-5 scheme, where we  
195 see the smallest areal distribution of gravelly sediments (1%), gravelly muddy Sands and gravelly Sands are grouped into  
196 the ‘Sands’ category. Gravels have additionally been observed at the southern entrance of the San Matías Gulf (Mouzo and  
197 Paterlini, 2017; Alonso, 2025), forming submerged dunes. We do not pick up these features, due to the spatial resolution  
198 of data available from the region.

199

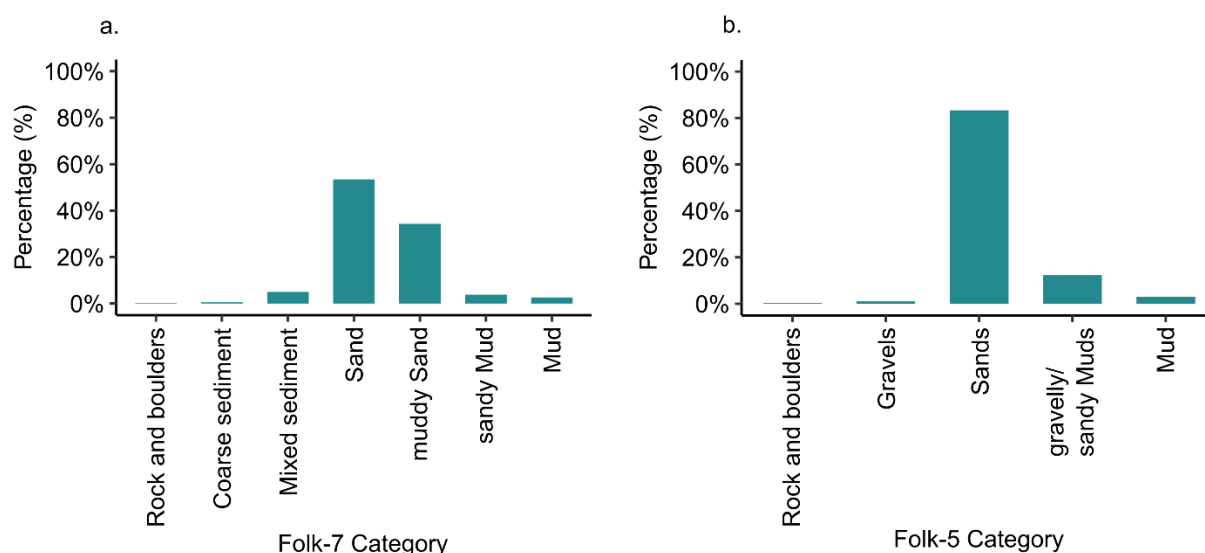
200 Considering that the data mining exercise carried out in this study is largely based on re-classified sediment descriptions,  
201 the discrepancies observed may be due to the subjective nature of both the original descriptions and their reclassification.  
202 We also note that the availability of seabed sediment data over the southern shelf is limited in places, with the error in  
203 prediction being relatively high around and to the west of Islas Malvinas/Falkland Islands; a sub-section of the shelf that  
204 is shown to be largely Gravel in previously published maps (Parker et al., 1996; Violante et al., 2014). Further sampling of  
205 surface sediments in this region, or further open-access publication of pre-existing substrate data/observations, would likely  
206 help refine the areal distribution of coarse sediments.

207

208 Muddy sediments are primarily found within inner shelf gulfs and estuaries of the Patagonian Shelf (Fig. 4 and 5; Violante  
209 et al., 2014). Following the Folk-7 scheme, 4% and 3% of the shelf is comprised of sandy Mud and Mud, respectively. We  
210 also find that 3% of shelf surface sediments are Mud (>90% Mud; Fig. 2), when using the Folk-5 scheme. Violante et al.  
211 (2014; after Parker et al., 1997) classify 8% of shelf sediments as ‘Muds’. As noted previously, the difference in areal  
212 extent (%) is likely due to the classification of sediment based on original descriptions and their reclassification, which are  
213 subjective in nature. However, the distribution of muddy sediments found in this study largely resembles previous maps  
214 (Parker et al., 1996; Violante et al., 2014). The largest bodies of muddy sediments on the shelf are found seawards of the  
215 Río de la Plata estuary and within San Jorge Gulf. The Río de la Plata estuary (Fig. 1a) is formed at the confluence of the  
216 Paraná and Uruguay Rivers. The Paraná River is the second longest river in South America, and carries a large, suspended  
217 load of fine sediments - clays and silts - into the estuary at a rate of  $160-200 \times 10^6 \text{ t yr}^{-1}$  (Fossati et al., 2014; Colombo et al.,



218 2021). Further fine sediments are supplied by the Uruguay River, which can reach a suspended load of  $\sim 100 \text{ mg L}^{-1}$  during  
219 high discharge events (Colombo et al., 2021). The San Jorge Gulf is not fed by any major rivers but receives sediment from  
220 the local coastline (40%) as well as through aeolian (10% dust) and oceanic transport (Desiagi et al., 2018). Lower energy  
221 hydrodynamic conditions within the central basin promote deposition of oceanic and aeolian-sourced fine sediment,  
222 relative to the coastal areas that receive a greater proportion of sediment through coastal erosion (Desiagi et al., 2018).  
223 Fine sediments (sandy Muds) are also found within Golfo San Matías, Golfo San José and Golfo Neuvo, and along the  
224 inner Patagonian Shelf south of Golfo San Jorge (Fray and Erwing, 1963; Violante et al., 2014).  
225



226  
227 **Figure 5: Areal coverage (%) of different sediment classes under the (a) Folk-7 and (b) Folk-5 schemes (Fig. 2).**

228  
229 Overall, the seabed sediment maps produced in this study, based on the harmonisation and interpolation of open-access  
230 data, agree well with previously published maps over the central and northern shelf. Key differences are the classification  
231 of shell-rich sediments, and the spatial distribution of coarse sediments particularly over the southern shelf. As noted, the  
232 areal extent of gravels could be resolved with greater availability of surficial sediment grain size data around and to the  
233 west of Islas Malvinas/Falkland Islands. More generally, our standard error of prediction maps highlight regions with  
234 sparse sample coverage (Fig. 3b and 4b) or high variability in sediment type. These areas would be of priority for further  
235 seabed sampling and would improve the coverage of open-access seabed grain size data for the Patagonian Shelf.

236



## 237 5. Data availability

238 All data compiled for this study are openly available via (Roseby et al., 2026; <https://doi.org/10.5281/zenodo.19111158>)  
239 and include:

- 240 • A polygon shapefile delimiting the area of interest
- 241 • The harmonised seabed sediment data set including information on: Site, Ship/Cruise, Year (of collection),  
242 Sampling method, Latitude, Longitude, Depth (metres below sea level), Grain size analysis methodology, Folk-7  
243 classification, Folk-5 classification, Surface sediment type (Folk description), Gravel (%), Sand (%), Mud (%),  
244 Author, DOI/source, Repository, Sediment description (from original core log), Notes, Quantitative (Yes/No). If  
245 metadata are unavailable cells show 'NA'.
- 246 • Georeferenced Tiff-file of the predicted sediment classes (Folk-5)
- 247 • Georeferenced Tiff-file of the standard error of prediction (Folk-5)
- 248 • Georeferenced Tiff-file of the predicted sediment classes (Folk-7)
- 249 • Georeferenced Tiff-file of the standard error of prediction (Folk-7)

250

## 251 6. Conclusions

252 Seabed sediment maps are of importance to several stakeholders, including those working in marine management and  
253 academic researchers. Whilst previous studies have produced surficial sediment maps for the Patagonian Shelf (Parker et  
254 al., 1996; Violante et al., 2014), no data source existed for compiled and harmonised open-access data. Furthermore,  
255 existing maps do not appear in a format which can be easily incorporated into Geographic Information System (GIS)  
256 software. In this study we collated both quantitative and qualitative data from published and grey literature, and harmonised  
257 these under two modified Folk schemes (Kaskela et al., 2014; Smeaton et al., 2021). Ordinary Kriging was deemed the  
258 most appropriate method for producing continuous seabed sediment maps of the shelf. These maps allowed us to assess  
259 the areal coverage of different sediment types and estimate uncertainty in our predictions. The collated and harmonised  
260 dataset, and GIS layers of seabed sediment type and associated prediction errors, are openly available via Roseby et al.  
261 (2026). Future work could incorporate bathymetric and backscatter data, whilst further sampling of data poor regions and/or  
262 further open-access publication of pre-existing seabed sediment data would likely help refine our understanding of the  
263 distribution of different seabed sediment types across the Patagonian Shelf.

264

265

266

267



268 **Author contribution**

269 ZR: Conceptualisation, data curation, formal analysis, investigation, methodology and writing (original draft preparation).

270 SW: Conceptualisation, writing (review and editing). JS: Conceptualisation, writing (review and editing). TS: Formal  
271 analysis, writing (review and editing). CR: Funding acquisition, writing (review and editing).

272

273 **Acknowledgements**

274 The authors acknowledge funding from Convex Group Ltd for the Convex Seascape Survey, which is facilitated by Blue  
275 Marine Foundation (<https://www.bluemarinefoundation.com/projects/convex-seascape-survey>)

276

277 **Competing interests**

278 The authors declare that they have no conflict of interest.

279

280 **References**

281 Alonso, G., Dragani, W. C., and Isla, F. I.: Reconstructing past tidal currents: A numerical approach to the paleotides of  
282 northern Patagonia, *Estuarine, Coastal and Shelf Science*, 326, 109536,  
283 <https://doi.org/10.1016/j.ecss.2025.109536>, 2025.

284 Atwood, T. B., Witt, A., Mayorga, J., Hammill, E., and Sala, E.: Global Patterns in Marine Sediment Carbon Stocks,  
285 *Frontiers in Marine Science*, 7, <https://doi.org/10.3389/fmars.2020.00165>, 2020.

286 Bernasconi, E. and Cusminsky, G.: Estudio paleoecológico de Foraminíferos de testigos del Holoceno de Golfo Nuevo  
287 (Patagonia, Argentina), *Geobios*, 42, 435-450, <https://doi.org/10.1016/j.geobios.2009.01.003>, 2009.

288 Boosman, J.W.: Depositional processes on the Argentine Continental Shelf. PhD Dissertation. George Washington  
289 University, 1973.

290 Boumpoulis, V., Michalopoulou, M., and Depountis, N.: Comparison between different spatial interpolation methods for  
291 the development of sediment distribution maps in coastal areas, *Earth Science Informatics*, 16, 2069-2087,  
292 <https://doi.org/10.1007/s12145-023-01017-4>, 2023.

293 Chaparro, M. A. E., Fernández, M., Chaparro, M. A. E., and Böhnell, H. N.: Magnetic proxies of continental shelf  
294 sediments and their implication for the benthic zone and shrimp fishing activities, *Continental Shelf Research*,  
295 248, 104845, <https://doi.org/10.1016/j.csr.2022.104845>, 2022.

296 Clark, P. U., Dyke, A. S., Shakun, J. D., Carlson, A. E., Clark, J., Wohlfarth, B., Mitrovica, J. X., Hostetler, S. W., and  
297 McCabe, A. M.: The Last Glacial Maximum, *Science*, 325, 710-714, <https://doi.org/10.1126/science.1172873>,  
298 2009.



- 299 Colombo, F., Serra, J., Cabello, P., Bedmar, J., and Isla, F. I.: Chronology of recent sedimentary infill of the Inner Río de  
300 la Plata Estuary, Argentina, *Journal of Iberian Geology*, 47, 663-684, [https://doi.org/10.1007/s41513-021-](https://doi.org/10.1007/s41513-021-00176-x)  
301 00176-x, 2021.
- 302 de Mahiques, M. M., Hanebuth, T. J. J., Martins, C. C., Montoya-Montes, I., Alcántara-Carrió, J., Figueira, R. C. L., and  
303 Bicego, M. C.: Mud depocentres on the continental shelf: a neglected sink for anthropogenic contaminants from  
304 the coastal zone, *Environmental Earth Sciences*, 75, 44, <https://doi.org/10.1007/s12665-015-4782-z>, 2015.
- 305 de Mahiques, M. M., Tassinari, C. C. G., Marcolini, S., Violante, R. A., Figueira, R. C. L., da Silveira, I. C. A., Burone,  
306 L., and de Mello e Sousa, S. H.: Nd and Pb isotope signatures on the Southeastern South American upper  
307 margin: Implications for sediment transport and source rocks, *Marine Geology*, 250, 51-63,  
308 <https://doi.org/10.1016/j.margeo.2007.11.007>, 2008.
- 309 Depetris, P. J. and J., G. J.: Suspended load in the Río de la Plata drainage basin, *Sedimentology*, 11, 53-60,  
310 <https://doi.org/10.1111/j.1365-3091.1968.tb00840.x>, 1968.
- 311 Desiagne, P.-A., St-Onge, G., Duchesne, M. J., Montero-Serrano, J.-C., and Haller, M. J.: Late Pleistocene and Holocene  
312 transgression inferred from the sediments of the Gulf of San Jorge, central Patagonia, Argentina, *Journal of*  
313 *Quaternary Science*, 38, <https://doi.org/10.1002/jqs.3511>, 2023.
- 314 Desiagne, P.-A., Montero-Serrano, J., St-Onge, G., Crespi-Abril, A., Giarratano, E., Gil, M., and Haller, M.: Quantifying  
315 Sources and Transport Pathways of Surface Sediments in the Gulf of San Jorge, Central Patagonia (Argentina),  
316 *Oceanography (Washington D.C.)*, 31, <https://doi.org/10.5670/oceanog.2018.401>, 2018.
- 317 Diesing, M., Thorsnes, T., and Bjarnadóttir, L. R.: Organic carbon densities and accumulation rates in surface sediments  
318 of the North Sea and Skagerrak, *Biogeosciences*, 18, 2139-2160, <https://doi.org/10.5194/bg-18-2139-2021>,  
319 2021.
- 320 Diesing, M., Paradis, S., Jensen, H., Thorsnes, T., Bjarnadóttir, L. R., and Knies, J.: Glacial troughs as centres of organic  
321 carbon accumulation on the Norwegian continental margin, *Communications Earth & Environment*, 5, 327,  
322 <https://doi.org/10.1038/s43247-024-01502-8>, 2024.
- 323 Doldan, M. S., Oehrens Kissner, E. M., Kroeck, M. A., and Morsan, E. M.: Population dynamics of the native oyster  
324 *Ostrea puelchana* d'Orbigny, 1842 in north-patagonian gulfs, Argentina: A multiscale spatial approach, *Marine*  
325 *Environmental Research*, 166, 105281, <https://doi.org/10.1016/j.marenvres.2021.105281>, 2021.
- 326 Esri: Choose the right projection, available from: <https://learn.arcgis.com/en/projects/choose-the-right-projection/>  
327 [Accessed 29 July 2025], 2025.



- 328 Fernández, M.: Características físico-químicas de los sedimentos del Golfo San Jorge y su relación con los organismos  
329 bentónico del sector, PhD Dissertation, Facultad de Ciencias Exactas y Naturales, Universidad Nacional de Mar  
330 del Plata, 2006.
- 331 Folk, R.L.: The Distinction between Grain Size and Mineral Composition in Sedimentary-Rock Nomenclature, The  
332 Journal of Geology, 62, 344-35, 1954.
- 333 Fossati, M., Cayocca, F., and Piedra-Cueva, I.: Fine sediment dynamics in the Río de la Plata, Adv. Geosci., 39, 75-80,  
334 <https://doi.org/10.5194/adgeo-39-75-2014>, 2014.
- 335 Fray, C., Erwing, M.: Pleistocene Sedimentation and Fauna of the Argentine Shelf: I. Wisconsin Sea Level as Indicated  
336 in Argentine Continental Shelf Sediments. Proceedings of the Academy of Natural Sciences of Philadelphia,  
337 115, 113-126, 1963.
- 338 GEBCO Compilation Group: GEBCO 2024 Grid, doi:10.5285/1c44ce99-0a0d-5f4f-e063-7086abc0ea0f, 2024.
- 339 Groeber, P.: Las plataformas submarinas y su edad, Revista Ciencia e investigación, 6, 224-231, 1948.
- 340 Guilderson, T., Burckle, L., Hemming, S., and Peltier, W.: Late Pleistocene sea level variations derived from the  
341 Argentine Shelf, Geochemistry, Geophysics, Geosystems, 1, <https://doi.org/10.1029/2000GC000098>, 2000.
- 342 JNCC: The Marine Habitat Classification for Britain and Ireland, Version 22.04, available from: <https://mhc.jncc.gov.uk/>  
343 [Accessed 29 July 2025], 2022.
- 344 Kaskela, A. M., Kotilainen, A. T., Alanen, U., Cooper, R., Green, S., Guinan, J., van Heteren, S., Kihlman, S., Van  
345 Lancker, V., Stevenson, A., and Partners, t. E. G.: Picking Up the Pieces—Harmonising and Collating Seabed  
346 Substrate Data for European Maritime Areas, Geosciences, 9, 84, <https://doi.org/10.3390/geosciences9020084>,  
347 2019.
- 348 Lantzsch, H., Hanebuth, T. J. J., Chiessi, C. M., Schwenk, T., and Violante, R. A.: The high-supply, current-dominated  
349 continental margin of southeastern South America during the late Quaternary, Quaternary Research, 81, 339-  
350 354, <https://doi.org/10.1016/j.yqres.2014.01.003>, 2014.
- 351 Liu, S., Shi, X., Liu, Y., Zhu, Z., Yang, G., Zhu, A., and Gao, J.: Concentration distribution and assessment of heavy  
352 metals in sediments of mud area from inner continental shelf of the East China Sea, Environmental Earth  
353 Sciences, 64, 567-579, <https://doi.org/10.1007/s12665-011-0941-z>, 2011.
- 354 Moreira, D., Simionato, C. G., Dragani, W., Cayocca, F., and Tejedor, M. L. C.: Characterization of Bottom Sediments  
355 in the Río de la Plata Estuary, Journal of Coastal Research, 32, 1473-1494, 1422,  
356 <https://doi.org/10.2112/JCOASTRES-D-15-00078.1>, 2016.
- 357 Mouzo, F. H., Paterlini, C. M.: Geología submarina del golfo norpatagónico San Matías. Revista De La Asociación  
358 Geológica Argentina, 74(4), 553-569, 2017.



- 359 Oliva, A. L., Quintas, P. Y., Ronda, A. C., Marcovecchio, J. E., and Arias, A. H.: First evidence of polycyclic aromatic  
360 hydrocarbons in sediments from a marine protected area within Argentinean Continental Shelf, *Marine Pollution*  
361 *Bulletin*, 158, 111385, <https://doi.org/10.1016/j.marpolbul.2020.111385>, 2020.
- 362 Palanques, A., Plana, F., and Maldonado, A.: Recent influence of man on the Ebro margin sedimentation system,  
363 northwestern Mediterranean Sea, *Marine Geology*, 95, 247-263, [https://doi.org/10.1016/0025-3227\(90\)90119-5](https://doi.org/10.1016/0025-3227(90)90119-5),  
364 1990.
- 365 Parker, G., Lanfredi, N. W., and Swift, D. J. P.: Seafloor response to flow in a southern hemisphere sand-ridge field:  
366 Argentine inner shelf, *Sedimentary Geology*, 33, 195-216, [https://doi.org/10.1016/0037-0738\(82\)90055-0](https://doi.org/10.1016/0037-0738(82)90055-0), 1982.
- 367 Parker, G., Paterlini, M., and Violante, R.: El fondo marino, in: *El Mar Argentino y sus Recursos Marinos*, vol. 1, edited  
368 by: Boschi, E.E., INIDEP, Mar del Plata, 65–87, 1997.
- 369 Parker, G., Violante, R., and Paterlini, C.: Fisiografía de la plataforma continental, *Geología y recursos naturales de la*  
370 *Plataforma Continental Argentina*, 1, 1-16, 1996.
- 371 Perillo, G., Piccolo, M., and Marcovecchio, J.: Coastal Oceanography of the Western South Atlantic continental shelf  
372 (33°S to 55°S), in: *The Sea: The Global Coastal Ocean, Regional studies and Syntheses*, edited by: En Robinson  
373 A.A., and Brink K., 295-327, 2005.
- 374 Ponce, J. F., Rabassa, J., Coronato, A., and Borromei, A. M.: Palaeogeographical evolution of the Atlantic coast of  
375 Pampa and Patagonia from the last glacial maximum to the Middle Holocene, *Biological Journal of the Linnean*  
376 *Society*, 103, 363-379, <https://doi.org/10.1111/j.1095-8312.2011.01653.x>, 2011.
- 377 Potter, P. E.: Modern sands of South America: composition, provenance and global significance, *Geologische*  
378 *Rundschau*, 83, 212-232, <https://doi.org/10.1007/BF00211904>, 1994.
- 379 Richards, A. F. and Dzwilewski, P. T.: Geotechnical properties of the Golfo San Matias, Argentina, *Journal of*  
380 *Sedimentary Research*, 44, 649-654, <https://doi.org/10.1306/74D72AB8-2B21-11D7-8648000102C1865D>,  
381 1974.
- 382 Robinson, K. A., Ramsay, K., Lindenbaum, C., Frost, N., Moore, J., Wright, A. P., and Petrey, D.: Predicting the  
383 distribution of seabed biotopes in the southern Irish Sea, *Continental Shelf Research*, 31, S120-S131,  
384 <https://doi.org/10.1016/j.csr.2010.01.010>, 2011.
- 385 Ronda, A. C., Arias, A. H., Oliva, A. L., and Marcovecchio, J. E.: Synthetic microfibers in marine sediments and surface  
386 seawater from the Argentinean continental shelf and a Marine Protected Area, *Marine Pollution Bulletin*, 149,  
387 110618, <https://doi.org/10.1016/j.marpolbul.2019.110618>, 2019.
- 388 Roseby, Z.A, Ward, S.L, Sengupta, T., Roberts, C.M, & Scourse, J.D.: Harmonising and mapping Patagonian Shelf  
389 seabed sediment data [Data set], Zenodo, <https://doi.org/10.5281/zenodo.19111158>, 2026.



- 390 Roux, A. and Bremec, C.: Brachiopoda collected in the western South Atlantic by R/V Shinkai Maru cruises (1978-  
391 1979), 1996.
- 392 Smeaton, C. and Austin, W. E. N.: Where's the Carbon: Exploring the Spatial Heterogeneity of Sedimentary Carbon in  
393 Mid-Latitude Fjords, *Frontiers in Earth Science*, Volume 7 - 2019, <https://doi.org/10.3389/feart.2019.00269>,  
394 2019.
- 395 Smeaton, C., Hunt, C. A., Turrell, W. R., and Austin, W. E. N.: Marine Sedimentary Carbon Stocks of the United  
396 Kingdom's Exclusive Economic Zone, *Frontiers in Earth Science*, Volume 9 - 2021,  
397 <https://doi.org/10.3389/feart.2021.593324>, 2021.
- 398 Tuduri, A., Bergamino, L., Violante, R., Cavallotto, J., and García-Rodríguez, F.: Spatial and temporal variation in the  
399 present and historical sedimentary organic matter within the Río de la Plata Estuary (South America) in relation  
400 to the salinity/turbidity gradient, *Journal of Sedimentary Environments*, 3,  
401 <https://doi.org/10.12957/jse.2018.39152>, 2019.
- 402 Violante, R.: Submerged terraces in the continental shelf of Argentina and its significance as paleo-sea level indicators:  
403 the example of the Rioplatense Terrace, 5th Annual conference Project IGCP, 97-99, 2005.
- 404 Violante, R., Paterlini, C., Marcolini, S., Costa, I., Cavallotto, J., Laprida, C., Dragani, W., Garcia Chaporí, N.,  
405 Watanabe, S., Totah, V., Rovere, E., and Osterrieth, M.: The Argentine continental shelf: morphology,  
406 sediments, processes and evolution since the Last Glacial Maximum, in: *Continental Shelves during the Last  
407 Glacio-eustatic Cycle: Shelves of the World*, edited by: Chiocci, F.L., and Chivas, A.R, Geological Society,  
408 London, *Memoirs*, 41, 55–68, <https://doi.org/10.1144/M41.6>, 2014.
- 409 Violante, R. A. and Parker, G.: The post-last glacial maximum transgression in the de la Plata River and adjacent inner  
410 continental shelf, Argentina, *Quaternary International*, 114, 167-181, [https://doi.org/10.1016/S1040-  
411 6182\(03\)00036-3](https://doi.org/10.1016/S1040-6182(03)00036-3), 2004.
- 412 Ward, S. L., Bradley, S. L., Roseby, Z. A., Wilmes, S.-B., Vosper, D. F., Roberts, C. M., and Scourse, J. D.: The Role of  
413 Long-Term Hydrodynamic Evolution in the Accumulation and Preservation of Organic Carbon-Rich Shelf Sea  
414 Deposits, *Journal of Geophysical Research: Oceans*, 130, e2024JC022092,  
415 <https://doi.org/10.1029/2024JC022092>, 2025.
- 416 Williams, M. E., Amoudry, L. O., Brown, J. M., and Thompson, C. E. L.: Fine particle retention and deposition in  
417 regions of cyclonic tidal current rotation, *Marine Geology*, 410, 122-134,  
418 <https://doi.org/10.1016/j.margeo.2019.01.006>, 2019.